Chemical Science

ROYAL SOCIETY OF CHEMISTRY

EDGE ARTICLE

View Article Online
View Journal | View Issue

Cite this: *Chem. Sci.*, 2024, **15**, 11965

All publication charges for this article have been paid for by the Royal Society of Chemistry

Received 12th May 2024
Accepted 14th June 2024

DOI: 10.1039/d4sc03104k

rsc.li/chemical-science

Multi-electron redox reactivity of a samarium(II) hydrido complex†

Xianghui Shi, [a] Peng Deng,[ab] Thayalan Rajeshkumar,[c] Laurent Maron *[c] and Jianhua Cheng *[ab]

Well-defined low-valent molecular rare-earth metal hydrides are rare, and limited to Yb^{2+} and Eu^{2+} centers. Here, we report the first example of the divalent samarium(II) hydrido complex $[(Cp^{Ar5})Sm^{II}(\mu\text{-}H)(DABCO)]_2$ (**4**) (Cp^{Ar5} = C_5Ar_5, Ar = 3,5-$^{i}Pr_2$-C_6H_3; DABCO = 1,4-diazabicyclooctane) supported by a super-bulky penta-arylcyclopentadienyl ligand, resulting from the hydrogenolysis of the samarium(II) alkyl complex $[(Cp^{Ar5})Sm^{II}\{CH(SiMe_3)_2\}(DABCO)]$ (**3**). Complex **4** exhibits multi-electron redox reactivity toward a variety of substrates. Exposure of complex **4** to CO_2 results in the formation of the trivalent samarium(III) mixed-bis-formate/carbonate complex $[(Cp^{Ar5})Sm^{III}(\mu\text{-}\eta^2{:}\eta^1\text{-}O_2CH)(\mu\text{-}\eta^2{:}\eta^2\text{-}CO_3)(\mu\text{-}\eta^1{:}\eta^1\text{-}O_2CH)Sm^{III}(Cp^{Ar5})(DABCO)]$ (**8**), mediated by hydride insertion and reductive disproportionation reactions. Complex **4** shows four-electron reduction toward four equivalents of CS_2 to afford the trivalent samarium(III) bis-trithiocarbonate complex $[(Cp^{Ar5})Sm^{III}(\mu\text{-}\eta^2{:}\eta^2\text{-}CS_3)(DABCO)]_2$ (**9**). A mechanistic study of the formation of complex **8** was carried out using DFT calculations.

Introduction

The chemistry of molecular hydrides of rare-earth metals has been extensively studied in the past four decades.[1] However, despite their significant roles in various stoichiometric and catalytic reactions, such complexes are dominated by trivalent rare-earth metal centers.[2] The difficulties in isolating discrete divalent rare-earth metal hydrides are mainly attributed to their greater ionic radii and higher reactivity levels, compared with trivalent rare-earth metals. So far, structurally characterized divalent rare-earth metal hydride species are scarce, consisting of a handful of ytterbium(II) hydrides[3–9] and three examples of europium(II) hydride complexes,[10] although all lanthanides(II), except for the radioactive promethium, are accessible in soluble molecules.[11] The Takats group reported the first example of a divalent ytterbium hydride complex $[(Tp^{tBu,Me})Yb(\mu\text{-}H)]_2$ ($Tp^{tBu,Me}$ = hydrotris(3-*tert*-butyl-5-methyl-pyrazolyl)borate) (Fig. 1, **I**).[3] The first mononuclear divalent ytterbium hydride complex bearing a terminal hydrido ligand—namely $[(Tp^{Ad,iPr})Yb(H)(THF)]$ ($Tp^{Ad,iPr}$ = hydrotris(3-adamantyl-5-isopropyl-pyrazolyl)borate) (Fig. 1, **II**)—was produced.[4] Three other ancillary ligand types (Fig. 1, **III–VI**) have been shown to stabilize neutral dimeric ytterbium hydrides, including the bulky ketiminate (BDI^{Dipp} = $(2,6\text{-}^{i}Pr_2C_6H_3)NC(Me)C(H)C(Me)N(2,6\text{-}^{i}Pr_2C_6H_3)$),[5,6] amidinate ($^{t}BuC(N\text{-}Dipp)_2$ = $(2,6\text{-}^{i}Pr_2C_6H_3)NC(^{t}Bu)N(2,6\text{-}^{i}Pr_2C_6H_3)$),[7] and β-diketiminato-based tetradentate ligand $(MeC(NDipp)CHC(Me)NCH_2CH_2N(Me)CH_2CH_2NMe_2$, Dipp = 2,6-$^{i}Pr_2$-$C_6H_3$).[8] Recently, Okuda and co-worker disclosed the first examples of cationic divalent ytterbium hydrides $[(Me_4\text{-}TACD)_2Yb_2(\mu\text{-}H)_{(2+n)}]^{(2-n)+}$ (n = 0, 1) (Me_4TACD = 1,4,7,10-tetramethyl-1,4,7,10-tetraazacyclododecane) (Fig. 1, **VII**).[9] Very recently, the bulky β-diketiminate ligand frameworks $\{BDI^{DCHP}\}^-$ and $[BDI^{Dipp/Ar}]^-$ (BDI = $[HC\{C(Me)_2N\text{-}Dipp/Ar\}_2]^-$ (Dipp = 2,6-$^{i}Pr_2$-C_6H_3; Ar = 2,6-Cy_2-C_6H_3 (DCHP) or 2,4,6-Cy_3-C_6H_2 (TCHP)) were developed for the kinetic stabilization of the first europium(II) hydride complexes (Fig. 1, **VIII**).[10]

Divalent ytterbium hydrides have been used in a variety of organic transformations, and the oxidation state of ytterbium center remains unchanged in most cases.[3–9,12] A more versatile chemistry can confidently be predicted for rare-earth metal hydrides with a highly reducing metal center.

Sm^{2+}, Yb^{2+} and Eu^{2+} have been classically regarded as the three most common Ln^{2+} examples in molecular lanthanide complexes in solution.[13] The Ln^{3+}/Ln^{2+} redox potentials for Sm^{2+}, Yb^{2+} and Eu^{2+} are, respectively, −1.55, −1.15 and −0.35 V *versus* NHE.[14] Divalent samarium complexes, for example, $Sm^{II}I_2(THF)_x$ (ref. 15) and $(Cp^*)_2Sm^{II}(THF)_x$ (Cp^* = C_5Me_5),[16] have been widely used as powerful electron-transfer reagents in various organic transformations. Compared with divalent

[a]*State Key Laboratory of Polymer Physics and Chemistry Changchun Institute of Applied Chemistry, Chinese Academy of Sciences, No. 5625, Renmin Street, Changchun 130022, China. E-mail: jhcheng@ciac.ac.cn*

[b]*School of Applied Chemistry and Engineering, University of Science and Technology of China, Hefei, Anhui, 230026, China*

[c]*LPCNO, CNRS & INSA, UPS, Université de Toulouse, 135 Avenue de Rangueil, 31077 Toulouse, France. E-mail: laurent.maron@irsamc.ups-tlse.fr*

† Electronic supplementary information (ESI) available: Experimental details, spectroscopic characterization. CCDC 2104460–2104466. For ESI and crystallographic data in CIF or other electronic format see DOI: https://doi.org/10.1039/d4sc03104k

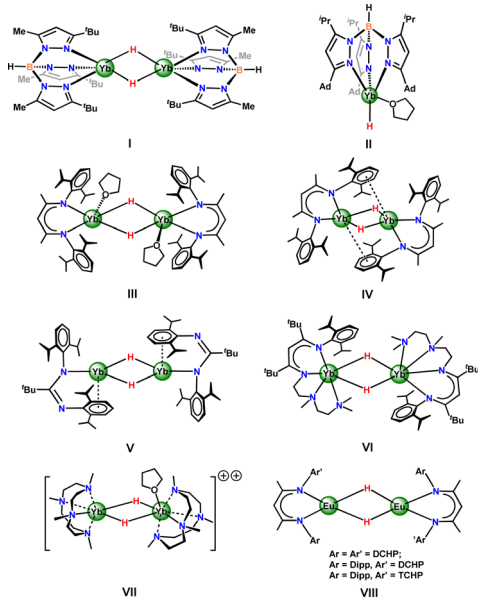

Fig. 1 Selected examples of divalent rare-earth metal hydride complexes.

ytterbium hydrides, the synthesis and structural characterization of divalent samarium hydrides are more challenging, because of the larger ionic radius (Yb^{2+} 1.02 Å, Sm^{2+} 1.17 Å; CN = 6),[17] and more reducing metal center and paramagnetic nature (Yb^{2+}: diamagnet; Sm^{2+}: 3.5–3.8 μ_B) of divalent samarium.[18] Molecular divalent samarium hydride complexes $[Sm^{II}H_2(THF)_2]$[19] and $[(Cp^*)Sm^{II}H(THF)_2]$[20] have been studied for decades, but no crystal structure has to date been obtained. Gambarotta *et al.* described an anionic divalent samarium hydride species, namely tetranuclear $\{([Ph_2C(C_4H_3N)_2]Sm^{II})_4(H)(THF)_2\}^-$, obtained serendipitously from the reduction of trivalent samarium precursor $\{[Ph_2C(C_4H_3N)_2]Sm^{III}Cl\}$ with sodium in THF. However, the hydride position in the crystal structure is elusive.[21] No further reactivity studies have been presented, as far as we know.

As the ionic radii of Sr^{2+} and Sm^{2+} are very similar (Sr^{2+} 1.18 Å, Sm^{2+} 1.17 Å; CN = 6),[17] there are strikingly similar interatomic parameters in their crystal structures.[22] Recently, our group found that the sterically demanding pentaarylcyclopentadienyl ligand Cp^{Ar5} (Cp^{Ar5} = C_5Ar_5, Ar = 3,5-^{i}Pr$_2$-C$_6$H$_3$)[23] can serve as an excellent ligand with the dinuclear structure.[23a] Encouraged by this success, we turned our attention to the synthesis of divalent samarium hydrides. Herein, we report the first example of a structural characterization of a neutral divalent samarium(II) hydrido complex, namely $[(Cp^{Ar5})Sm^{II}(\mu\text{-}H)(DABCO)]_2$ (**4**), generated from a moderate-pressure (20 atm) hydrogenolysis of the corresponding samarium(II) alkyl precursor. Preliminarily determined reactivities of divalent samarium(II) hydrides with Se, azobenzene (PhN=NPh), CO_2, and CS_2 are presented as well.

Results and discussion

As the precursor of reported strontium hydrides, the strontium alkyl complex $[(Cp^{Ar5})Sr\{CH(SiMe_3)_2\}(THF)]$[23a] was generated from the reaction of $(Cp^{Ar5})H$ with $[Sr\{CH(SiMe_3)_2\}_2(THF)_2]$.[24] However, the samarium analogue "$[Sm^{II}\{CH(SiMe_3)_2\}_2(THF)_2]$" is inaccessible. Protonolysis reactions of $(Cp^{Ar5})H$ with samarium benzyl complexes, for example $[Sm^{II}_2(CH_2Ph)_4(THF)_3]$[25] and $[(DMAT)_2Sm^{II}(THF)]$ (DMAT = 2-Me$_2$N-α-Me$_3$Si-benzyl),[24,26] failed. Thus, two-step salt metathesis reactions were carried out (Scheme 1). Treatment of $(Cp^{Ar5})K(THF)_2$ (**1**) with $[Sm^{II}I_2(THF)_5]$[27] in tetrahydropyran (THP), followed by the exchange of coordinated THP with DABCO, afforded the heteroleptic divalent samarium(II) iodide complex $[(Cp^{Ar5})Sm^{II}(\mu\text{-}I)(DABCO)]_2$ (**2**) as dark-green crystals in 92% isolated yield. Reaction of complex **2** with $KCH(SiMe_3)_2$ (ref. 28) in benzene gave the half-sandwich samarium(II) alkyl complex $[(Cp^{Ar5})Sm^{II}\{CH(SiMe_3)_2\}(DABCO)]$ (**3**) as a dark-brown solid in 86% isolated yield. Due to the high solubility of complex **3** in hydrocarbon solvents such as hexane, no crystallographically definable product could be isolated.

Hydrogenolysis of complex **3** in hexane under 20 atm H_2 successfully afforded the corresponding hydride complex $[(Cp^{Ar5})Sm^{II}(\mu\text{-}H)(DABCO)]_2$ (**4**) as dark-brown crystals in 78% isolated yield (Scheme 1), concomitant with $CH_2(SiMe_3)_2$. Complex **4** was found to be slightly soluble in hexane, and quite soluble in benzene. Complex **4** decomposed completely in C_6D_6 within two days and converted quickly to samarocene $[(Cp^{Ar5})_2Sm^{II}]$ (**5**) in THF through ligand redistribution at room temperature. The molecular structure of complex **5** (ESI, Fig. S32†) was observed to be similar to those of other decaarylsamarocenes $[\{C_5(4\text{-}R\text{-}C_6H_4)_5\}_2Sm^{II}]$ (R = Et, *n*-Bu).[22,29]

The ^{1}H NMR spectrum of complex **4** showed very broad signals, attributed to the paramagnetic nature of the Sm^{2+} ion, and hence could not be fully assigned. However, a signal attributed to bridging hydrides was observed at 1.63 ppm, corroborated by a ^{2}H NMR spectrum for the deuterated analogue $[(Cp^{Ar5})Sm^{II}(\mu\text{-}D)(DABCO)]_2$ (**4-D**). Based on magnetic measurements, the magnetic moments of complexes **2** and **4** at 300 K were measured to be 3.2 μ_B and 3.9 μ_B, respectively, consistent with divalent samarium derivatives.[18]

The dimeric nature of complex **4** in the solid state was revealed by X-ray crystallographic studies to be isostructural to $[(Cp^{Ar5})Sr(\mu\text{-}H)(DABCO)]_2$. Each Sm^{2+} center coordinated with one η^5-Cp^{Ar5} ligand, one DABCO ligand and two bridging hydrido ligands. The bridging hydrido ligand H1 was located using difference Fourier syntheses and refined isotopically

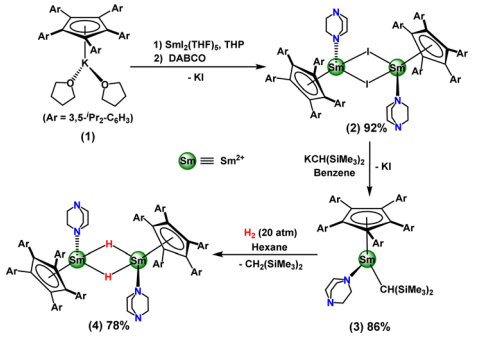

Scheme 1 Synthesis of the divalent samarium(II) hydride **4**.

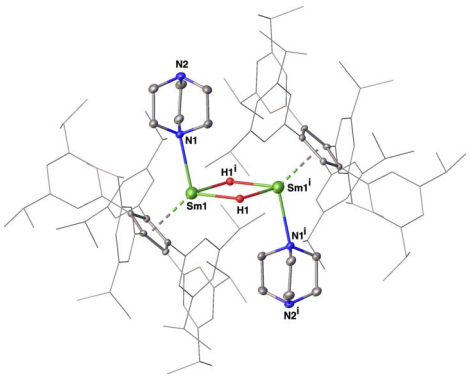

Fig. 2 Molecular structure of complex **4**. All the hydrogen atoms except the bridging hydrides (H1 and H1^{i}) are omitted for clarity. Selected interatomic distances [Å] and angles [deg]: Sm1–H1 2.26(6), Sm1–N1 2.652 (4), Sm1–Cent1 2.594, Sm1–Sm1^{i} 3.7966 (5), Sm1–H1–Sm1^{i} 106 (2), H1–Sm1–H1^{i} 74 (2). Cent: center of the Cp^{Ar5} ring.

(Fig. 2). Analysis of the structure showed Sm1–N1 (2.652(4) Å), Sm1–Cent1 (2.594 Å) and Sm1–Sm1^{i} (3.7966(5) Å) bond distances almost identical to those in [(Cp^{Ar5})Sr(μ-H)(DABCO)]$_2$,[23a] and showed Sm–H distances, of 2.26(6) Å and 2.48(5) Å, in the range (2.26(5)–2.86(6) Å) found in the molecular strontium hydride complexes.[23a,30] Thus, our work with complex **4** yielded the first example of a structurally characterized Sm(II) hydride complex, in comparison to the dozen previously reported examples of trivalent samarium(III) hydrides.[31]

As shown in Scheme 2, complex **4** readily reduced two equivalents of elemental Se in an apparent four-electron reduction to afford the corresponding trivalent samarium complex [(Cp^{Ar5})Sm^{III}(μ-Se)(DABCO)]$_2$ (**6**) in 77% isolated yield, with the four-electron reduction formally involving two one-electron hydride reductions and two one-electron Sm^{2+}/Sm^{3+} reductions. Here, a distinct change in the color of the benzene solution from dark brown to pale brown was observed instantly, in company wih the release of H_2.

Structural analyses showed the molecular framework of complex **6** to be similar to that of complex **2**, except for the bridging atoms and the oxidation state of Sm centers (ESI, Fig. S30 and S33†), and showed the bond lengths of Sm–Se (2.7349(7)~2.7524(6) Å) in complex **6** to be comparable to those in samarium complex [(Cp*)$_2$Sm^{III}(THF)]$_2$(μ-Se) (2.782(1) and 2.779(1) Å).[32]

Complex **4** also apparently acted as a four-electron reductant in the reduction of 2 equivalents of PhN=NPh to give [(Cp^{Ar5})Sm^{III}(μ-PhN-NPh)]$_2$ (**7**) as a red-brown solid in a measured 89% isolated yield. As shown in Fig. S34,† the N1–N2 bond length (1.462(3) Å) in the [PhN-NPh]$^{2-}$ unit was found to be comparable to that of the previously reported samarium(III) complex [(Cp*)Sm^{III}(μ-PhN-NPh)(THF)]$_2$ (1.44(1) Å).[33a] In contrast, Evans and coworkers reported the reductive cleavage of azobenzene into uranium(VI) bis(imido) complex (Cp*)$_2$U(NPh)$_2$.[33b]

Rare-earth metal complexes have been found to engage in extensive chemistry with carbon dioxide (CO_2)[34] and carbon disulfide (CS_2).[35] Exposure of a solution of complex **4** in toluene to 1 atm of CO_2 resulted in a decolorization to pale yellow in 30 minutes. The trivalent-samarium mixed-bis-formate/carbonate complex [(Cp^{Ar5})Sm^{III}(μ-η^2:η^1-O$_2$CH)(μ-η^2:η^2-CO$_3$)(μ-η^1:η^1-O$_2$CH)Sm^{III}(Cp^{Ar5})(DABCO)] (**8**) was isolated from a hexane solution as pale-yellow crystals in 75% yield (Scheme 3).

Due to the paramagnetic nature of complex **8**, no meaningful data could be obtained from its ^{1}H and ^{13}C NMR spectra. Accordingly, the solid-state structure of compound **8** was determined using X-ray crystallography and is highlighted in Fig. 3. Inspection of this structure showed two [(Cp^{Ar5})Sm^{III}] fragments bridged by one carbonate [CO$_3$]$^{2-}$ ligand and two formate [O$_2$CH]$^-$ moieties. It specifically showed the bridging carbonate [CO$_3$]$^{2-}$ unit symmetrically bonded to the metal centers in a μ-η^2:η^2 mode, with similar Sm–O bond distances (Sm1–O3, 2.397(3) Å; Sm2–O3, 2.398(3) Å) and Sm–O–C bond angles (Sm1–O3–C1, 88.2(3)°; Sm2–O3–C1, 91.0(3)°)—but showed unequal C–O bond lengths in the carbonate unit, specifically with C1–O1 (1.204(6) Å) and C1–O2 (1.251(6) Å) being significantly shorter than C1–O3 (1.349(8) Å). Two different coordination patterns for the [O$_2$CH]$^-$ moieties were observed: one being a μ-η^1:η^1 mode, and the other a μ-η^2:η^1 mode, different from previously reported rare-earth metal formate complexes.[36] The coordination sphere of Sm1 was completed by a DABCO ligand, to have the same coordination number as that of the Sm2 center. Other interatom bond distances, *e.g.*, Sm1–N1 (2.605(3) Å) and Sm–Cent (2.523 and 2.452 Å), were found to be in agreement with trivalent samarium(III) complexes **6** and **7**.

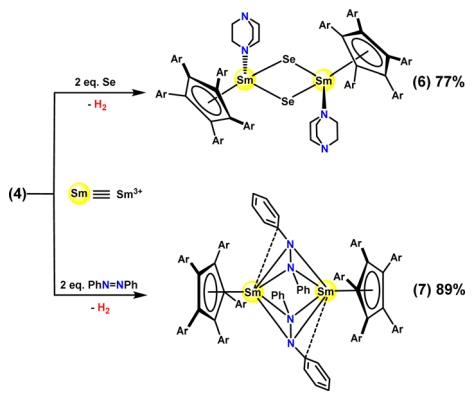

Scheme 2 Reactions of complex **4** with Se and azobenzene.

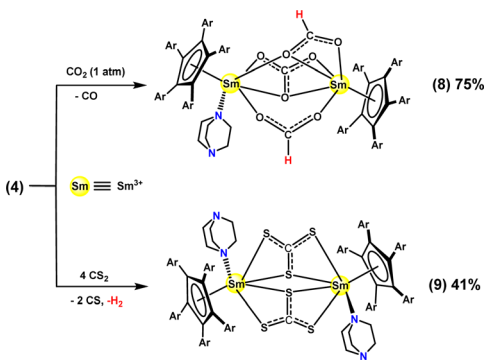

Scheme 3 Reactions of complex **4** with CO_2 and CS_2.

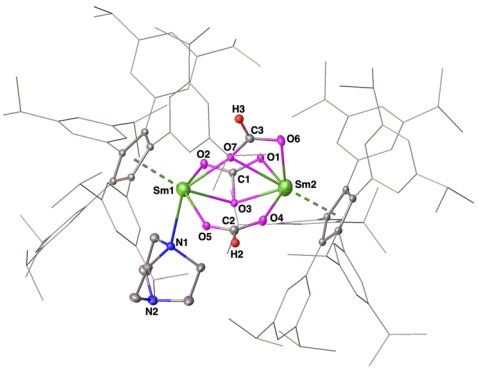

Fig. 3 Molecular structure of complex **8**. All the hydrogen atoms, except H2 and H3, are omitted for clarity. Selected interatomic distances [Å] and angles [deg]: Sm1–O2 2.354(2), Sm1–O3 2.397(3), Sm1–O5 2.338(2), Sm1–O7 2.426(2), Sm1–N1 2.605(3), Sm2–O1 2.373(3), Sm2–O3 2.398(3), Sm2–O4 2.346(2), Sm2–O6 2.406(3), Sm2–O7 2.644(2), C1–O1 1.251 (6), C1–O2 1.204(6), C1–O3 1.349(8), C2–O4 1.248(7), C2–O5 1.206(7), C3–O6 1.249(5), C3–O7 1.271(4), Sm1–Cent1 2.523, Sm2–Cent2 2.453, O2–C1–O1 133.6(6), O2–C1–O3 112.1(5), O1–C1–O3 113.8(5), O5–C2–O4 133.1(7), O6–C3–O7 121.7(4). Cent: center of the Cp^{Ar5} ring.

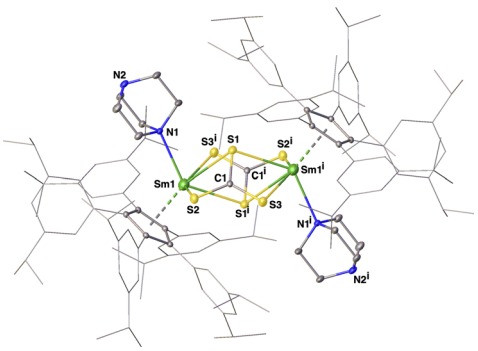

Fig. 4 Molecular structure of complex **9**. All the hydrogen atoms are omitted for clarity. Selected interatomic distances [Å] and angles [deg]: Sm1–S1 2.9774(8), Sm1–S2 2.8243(8), Sm1–$S3^i$ 2.8393(8), C1–S1 1.726(3), C1–S2 1.698(3), C1–S3 1.705(3), Sm1–N1 2.581(3), Sm1–Cent1 2.518, S1–C1–S2 118.35(17), S1–C1–S3 119.28(17), S2–C1–S3 122.29(19). Cent1: center of the Cp^{Ar5} ring.

Apparently, four equivalents of CO_2 were involved in this reaction. Two CO_2 molecules inserted into Sm–H bonds to form two formate units with different bonding modes. The other two CO_2 molecules likely underwent two-electron reduction and disproportionation to generate carbonate species $[CO_3]^{2-}$ with the release of carbon monoxide (CO), which has been proposed in the formation of other rare-earth metal carbonate complexes.[37]

Treatment of complex **4** with CS_2 in toluene gave a red-brown solution in 30 minutes. Trivalent samarium bis-trithiocarbonate complex $[(Cp^{Ar5})Sm^{III}(\mu\text{-}\eta^2\text{:}\eta^2\text{-}CS_3)(DABCO)]_2$ (**9**) was isolated as red-brown crystals in 41% yield. The whole molecule was determined according to X-ray crystallographic studies to adopt a binuclear structure composed of two Cp^{Ar5}-supported samarium trithiocarbonate units (Fig. 4), with each Sm^{3+} center coordinated with one η^5-Cp^{Ar5} ligand, one DABCO ligand and two bridging μ-η^2:η^2-CS_3 ligands. It was obvious that this reaction occurred with the oxidation of both Sm(II) and hydrido centers, and the reductive disproportionation of four equivalents of CS_2 to give two trithiocarbonate $[CS_3]^{2-}$ units with the release of carbon monosulfide (CS). Note the generation of $[CS_3]^{2-}$ species through a two-electron reduction in complex **4** being comparable to that previously reported for a rare-earth metal trithiocarbonate complex.[38]

In order to gain more insights into the previously unobserved reactivity of complex **4** toward CO_2, DFT calculations (B3PW91) were carried out (Fig. 5). According to these calculations, the reaction begins with the insertion of a CO_2 molecule into a Sm–H bond, *via* **TS1** and an activation barrier of 12.2 kcal mol^{-1}, a value typical of an insertion of a double-bond into to a Ln–H bond. The reaction then yields a very stable formate-hydride di-samarium(II) intermediate (**Int2**), with the formate ligand in this complex μ^2-bonded to the two Sm centers. A second CO_2 molecule is readily inserted into this intermediate with a very low barrier (5.1 kcal mol^{-1}) to form the bisformate di-samarium(II) intermediate (**Int3**), calculated to be thermodynamically highly stable (−113.4 kcal mol^{-1}). **Int3** then reacts with a third molecule of CO_2 in an expected redox fashion. Indeed, each of the two Sm(II) centers undergoes a single electron transfer (SET) to CO_2, which becomes doubly

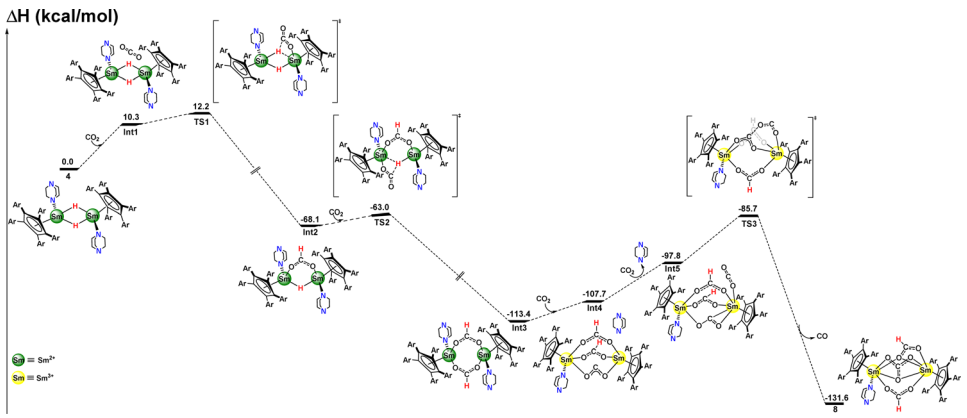

Fig. 5 Computed enthalpy profile for the reaction of **4** with four equivalents of CO_2 at room temperature. The energies are given in kcal mol^{-1}.

reduced, and each Sm center becomes oxidized to +III. This intermediate (**Int4**), usually called the "key intermediate" in SET reactions, adopts a dioxocarbene form as previously reported by Paparo *et al.* in titanium chemistry.[39] This step is slightly endothermic, by 5.7 kcal mol^{-1}, so that **Int4** is expected to be quite reactive. Thus, **Int4** readily reacts with a fourth molecule of CO_2, with this reaction implying the release of one DABCO molecule to allow CO_2 to bind to one Sm(III) center (**Int5**). This ligand exchange is endothermic by 9.9 kcal mol^{-1} from **Int4**, that is 15.6 kcal mol^{-1} from **Int3**. Then from **Int5**, a C–O bond formation occurs between the doubly reduced CO_2 and the other CO_2 molecule (bonded to Sm) *via* **TS3**—with an associated barrier of 12.1 kcal mol^{-1} from **Int5**, that is 27.7 kcal mol^{-1} from **Int3**, in line with a kinetically accessible reaction. Finally according to the calculations, the formation of the C–O bond allows the formation of the carbonate ligand and the release of a CO molecule, as observed in complex **8**, with the formation of this complex being highly exothermic (−131.6 kcal mol^{-1}).

Conclusions

In summary, we have demonstrated a synthesis, isolation and structural characterization of dimeric divalent samarium hydrido complex **4** bearing a super-bulky pentaarylcyclopentadienyl ligand. Complex **4** showed four-electron reduction toward various substrates, including Se, PhN=NPh and CS_2, to afford the corresponding double Se^{2-}, $[PhN\text{-}NPh]^{2-}$, and $[CS_3]^{2-}$ bridged trivalent samarium complexes, respectively, without suffering from ligand loss or ligand scrambling. For comparison, hydride insertion and two-electron reductive disproportionation of CO_2 were observed in the formation of mixed-bis-formate/carbonate complex **8**, corroborated by DFT calculations. These preliminarily determined reactivities indicate that complex **4** can provide an entry into an exciting new area involving the cooperation of a highly reactive hydride and a strong reducing metal center.

Data availability

All data (experimental procedures and characterization) that support the findings of this study are available within the article and its ESI.† Crystallographic data for complexes **2**, **4–9** have been deposited with the Cambridge Crystallographic Data Centre under CCDC 2104460–2104466.

Author contributions

X. S. carried out the synthesis and characterization of complexes **1–9**. P. D. assisted in the NMR spectroscopy experiment and crystal structure analysis. T. R. and L. M. performed the theoretical calculations. J. C. conceived this project and provided guidance. The manuscript was written with contributions from all the authors.

Conflicts of interest

The authors declare no conflict of interest.

Acknowledgements

This work was supported by the National Natural Science Foundation of China (No. 21901238 and 22271272). L. M. is a senior member of the Institut Universitaire de France. The Chinese Academy of Science is acknowledged for financial support (LM) and CalMip for a generous grant of computing time.

Notes and references

1 (*a*) M. Ephritikhine, *Chem. Rev.*, 1997, **97**, 2193; (*b*) F. T. Edelmann in *Comprehensive Organometallic Chemistry III*, ed. R. H. Crabtree and D. M. P. Mingos, Elsevier, Oxford, 2006, vol. 4.01, p. 1; (*c*) M. Nishiura and Z. Hou, *Nat. Chem.*, 2010, **2**, 257; (*d*) A. A. Trifonov and D. M. Lyubov, *Coord. Chem. Rev.*, 2017, **340**, 10; (*e*) T. Shima and Z. Hou, in *Recent Development in Clusters of Rare Earths and Actinides: Chemistry and Materials*, ed. Z. Zheng, Springer, Berlin, Heidelberg, 2017, p. 315; (*f*) W. J. Evans, J. H. Meadows, A. L. Wayda, W. E. Hunter and J. L. Atwood, *J. Am. Chem. Soc.*, 1982, **104**, 2008.

2 Recent reviews of trivalent rare-earth metal hydrides, see: (*a*) Z. Hou, M. Nishiura and T. Shima, *Eur. J. Inorg. Chem.*, 2007, 2535; (*b*) M. Konkol and J. Okuda, *Coord. Chem. Rev.*, 2008, **252**, 1577; (*c*) A. A. Trifonov, *Coord. Chem. Rev.*, 2010, **254**, 1327; (*d*) W. Fegler, A. Venugopal, M. Kramer and J. Okuda, *Angew. Chem., Int. Ed.*, 2015, **54**, 1724; (*e*) J. Cheng, K. Saliu, M. J. Ferguson, R. McDonald and J. Takats, *J. Organomet. Chem.*, 2010, **695**, 2696; (*f*) J. Okuda, *Coord. Chem. Rev.*, 2017, **340**, 2.

3 (*a*) G. M. Ferrence, R. McDonald and J. Takats, *Angew. Chem., Int. Ed.*, 1999, **38**, 2233; (*b*) G. M. Ferrence and J. Takats, *J. Organomet. Chem.*, 2002, **647**, 84.

4 (*a*) X. Shi, P. Deng, T. Rajeshkumar, L. Zhao, L. Maron and J. Cheng, *Chem. Commun.*, 2021, **57**, 10047; (*b*) X. Shi, T. Rajeshkumar, L. Maron and J. Cheng, *Chem. Commun.*, 2022, **58**, 1362.

5 C. Ruspic, J. Spielmann and S. Harder, *Inorg. Chem.*, 2007, **46**, 5320.

6 (*a*) G. M. Richardson, I. Douair, S. A. Cameron, J. Bracegirdle, R. A. Keyzers, M. S. Hill, L. Maron and M. D. Ankder, *Nat. Commun.*, 2021, **12**, 3147; (*b*) G. M. Richardson, I. Douair, S. A. Cameron, L. Maron and M. D. Ankder, *Chem.–Eur. J.*, 2021, **27**, 13144; (*c*) G. M. Richardson, J. Howarth, M. J. Evans, A. J. Edwards, S. A. Cameron and M. D. Anker, *J. Coord. Chem.*, 2022, **75**, 1954.

7 (*a*) I. V. Basalov, D. M. Lyubov, G. K. Fukin, A. S. Shavyrin and A. A. Trifonov, *Angew. Chem., Int. Ed.*, 2012, **51**, 3444; (*b*) I. V. Basalov, D. M. Lyubov, G. K. Fukin, A. V. Cherkasov and A. A. Trifonov, *Organometallics*, 2013, **32**, 1507; (*c*) D. M. Lyubov, I. V. Basalov, A. S. Shavyrin, A. V. Cherkasov and A. A. Trifonov, *Russ. J. Coord. Chem.*, 2019, **45**, 728; (*d*) D. O. Khristolyubov, D. M. Lyubov and A. A. Trifonov, *Russ. Chem. Rev.*, 2021, **90**, 529.

8 (*a*) Q. Wen, B. Feng, L. Xiang, X. Leng and Y. Chen, *Inorg. Chem.*, 2021, **60**, 13913; (*b*) Q. Wen, T. Rajeshkumar, L. Maron, X. Leng and Y. Chen, *Angew. Chem., Int. Ed.*, 2022, **61**, e202200540.

9 D. Schuhknecht, K. N. Truong, T. P. Spaniol, L. Maron and J. Okuda, *Chem. Commun.*, 2018, **54**, 11280.
10 G. M. Richardson, M. J. Evans, T. Rajeshkumar, J. A. J. McCone, S. A. Cameron, L. Maron, C. Jones and M. D. Anker, *Chem.–Eur. J.*, 2024, e202400681.
11 M. R. MacDonald, J. E. Bates, J. W. Ziller, F. Furche and W. J. Evans, *J. Am. Chem. Soc.*, 2013, **135**, 9857.
12 (*a*) Y. Shi, J. Li and C. Cui, *Dalton Trans.*, 2017, **46**, 10957; (*b*) X. Liu, L. Xiang, E. Louyriac, L. Maron, X. Leng and Y. Chen, *J. Am. Chem. Soc.*, 2019, **141**, 138.
13 W. J. Evans, *Organometallics*, 2016, **35**, 3088.
14 W. J. Evans, *Coord. Chem. Rev.*, 2000, **206–207**, 263.
15 (*a*) D. J. Procter, R. A. I. I. Flowers and T. Skrydstrup, *Organic Synthesis using Samarium Diiodide: A Practical Guide*, RSC Publishing, Cambridge, 2009; (*b*) K. Gopalaiah and H. B. Kagan, *Chem. Rec.*, 2013, **13**, 187; (*c*) M. Szostak, N. J. Fazakerley, D. Parmar and D. J. Procter, *Chem. Rev.*, 2014, **114**, 5959.
16 (*a*) W. J. Evans, I. Bloom, W. E. Hunter and J. L. Atwood, *J. Am. Chem. Soc.*, 1981, **103**, 6507; (*b*) W. J. Evans, L. A. Hughes and T. P. Hanusa, *J. Am. Chem. Soc.*, 1984, **106**, 4270; (*c*) W. J. Evans, *Inorg. Chem.*, 2007, **46**, 3435; (*d*) C. Schoo, S. Bestgen, A. Egeberg, J. Seibert, S. N. Konchenko, C. Feldmann and P. W. Roesky, *Angew. Chem., Int. Ed.*, 2019, **58**, 4386; (*e*) A. J. Ryan and W. J. Evans, in *Structure and Bonding*, ed. D. M. P. Mingos, 2019, vol. 181, p. 197, and references therein.
17 R. D. Shannon, *Acta Crystallogr., Sect. A: Cryst. Phys., Diffr., Theor. Gen. Crystallogr.*, 1976, **32**, 751.
18 W. J. Evans and M. A. Hozbor, *J. Organomet. Chem.*, 1987, **326**, 299.
19 E. A. Fedorova, A. A. Trifonov, E. N. Kirillov and M. N. Bochkarev, *Russ. Chem. Bull.*, 2000, **49**, 946.
20 W. J. Evans, I. Bloom, W. E. Hunter and J. L. Atwood, *Organometallics*, 1985, **4**, 112.
21 T. Dube, M. Ganesan, S. Conoci, S. Gambarotta and G. P. A. Yap, *Organometallics*, 2000, **19**, 3716.
22 (*a*) S. Harder, *Angew. Chem., Int. Ed.*, 2004, **43**, 2714; (*b*) L. Orzechowski, D. F. J. Piesik, C. Ruspic and S. Harder, *Dalton Trans.*, 2008, 4742; (*c*) S. Harder, D. Naglav, C. Ruspic, C. Wickleder, M. Adlung, W. Hermes, M. Eul, R. Pottgen, D. B. Rego, F. Poineau, K. R. Czerwinski, R. H. Herber and I. Nowik, *Chem.–Eur. J.*, 2013, **19**, 12272.
23 (*a*) X. Shi, G. Qin, Y. Wang, L. Zhao, Z. Liu and J. Cheng, *Angew. Chem., Int. Ed.*, 2019, **58**, 4356; (*b*) Y. Wang and J. Cheng, *New J. Chem.*, 2020, **44**, 17333; (*c*) Y. Wang, I. K. Del, G. Qin, L. Zhao, L. Maron, X. Shi and J. Cheng, *Chem. Commun.*, 2021, **57**, 7766; (*d*) L. Zhao, P. Deng, X. Gong, X. Kang and J. Cheng, *ACS Catal.*, 2022, **12**, 7877.
24 M. R. Crimmin, A. G. M. Barrett, M. S. Hill, D. J. MacDougall, M. F. Mahon and P. A. Procopiou, *Chem.–Eur. J.*, 2008, **14**, 11292.
25 B. M. Wolf, C. Stuhl and R. Anwander, *Chem. Commun.*, 2018, **54**, 8826.
26 N. J. C. van Velzen and S. Harder, *Organometallics*, 2018, **37**, 2263.
27 (*a*) P. Girard, J. L. Namy and H. B. Kagan, *J. Am. Chem. Soc.*, 1980, **102**, 2693; (*b*) W. J. Evans, T. S. Gummersheimer and J. W. Ziller, *J. Am. Chem. Soc.*, 1995, **117**, 8999.
28 P. B. Hitchcock, A. V. Khvostov and M. F. Lappert, *J. Organomet. Chem.*, 2002, **663**, 263.
29 C. Ruspic, J. R. Moss, M. Schurmann and S. Harder, *Angew. Chem., Int. Ed.*, 2008, **47**, 2121.
30 (*a*) B. Maitland, M. Wiesinger, J. Langer, G. Ballmann, J. Pahl, H. Elsen, C. Färber and S. Harder, *Angew. Chem., Int. Ed.*, 2017, **56**, 11880; (*b*) C. N. de Bruin-Dickason, T. Sutcliffe, C. A. Lamsfus, G. B. Deacon, L. Maron and C. Jones, *Chem. Commun.*, 2018, **54**, 786; (*c*) D. Mukherjee, T. Hollerhage, V. Leich, T. P. Spaniol, U. Englert, L. Maron and J. Okuda, *J. Am. Chem. Soc.*, 2018, **140**, 3403; (*d*) B. Rösch, T. X. Gentner, H. Elsen, C. A. Fischer, J. Langer, M. Wiesinger and S. Harder, *Angew. Chem., Int. Ed.*, 2019, **58**, 5396; (*e*) J. Martin, J. Eyselein, J. Langer, H. Elsen and S. Harder, *Chem. Commun.*, 2020, **56**, 9178; (*f*) T. Hollerhage, A. Carpentier, T. P. Spaniol, L. Maron, U. Englert and J. Okuda, *Chem. Commun.*, 2021, **57**, 6316; (*g*) T. Hoellerhage, T. P. Spaniol, A. Carpentier, L. Maron and J. Okuda, *Inorg. Chem.*, 2022, **61**, 3309; (*h*) T. Hollerhage, P. Ghana, T. P. Spaniol, A. Carpentier, L. Maron, U. Englert and J. Okuda, *Angew. Chem., Int. Ed.*, 2022, **61**, e202115379.
31 (*a*) W. J. Evans, I. Bloom, W. E. Hunter and J. L. Atwood, *J. Am. Chem. Soc.*, 1983, **105**, 1401; (*b*) Y. K. Gunko, B. M. Bulychev, G. L. Soloveichik and V. K. Belsky, *J. Organomet. Chem.*, 1992, **424**, 289; (*c*) G. Desurmont, Y. Li, H. Yasuda, T. Maruo, N. Kanehisa and Y. Kai, *Organometallics*, 2000, **19**, 1811; (*d*) A. A. Trifonov, G. G. Skvortsov, D. M. Lyubov, N. A. Skorodumova, G. K. Fukin, E. V. Baranov and V. N. Glushakova, *Chem.–Eur. J.*, 2006, **12**, 5320; (*e*) J. Cheng, K. Saliu, G. Y. Kiel, M. J. Ferguson, R. McDonald and J. Takats, *Angew. Chem., Int. Ed.*, 2008, **47**, 4910; (*f*) M. Nishiura, J. Baldamus, T. Shima, K. Mori and Z. Hou, *Chem.–Eur. J.*, 2011, **17**, 5033; (*g*) D. Martin, J. Kleemann, E. Abinet, T. P. Spaniol, L. Maron and J. Okuda, *Eur. J. Inorg. Chem.*, 2013, 3987; (*h*) J. Liu, W. Chen, J. Li and C. Cui, *ACS Catal.*, 2018, **8**, 2230.
32 W. J. Evans, G. W. Rabe, J. W. Ziller and R. J. Doedens, *Inorg. Chem.*, 1994, **33**, 2719.
33 (*a*) W. J. Evans, D. K. Drummond, L. R. Chamberlain, R. J. Doedens, S. G. Bott, H. M. Zhang and J. L. Atwood, *J. Am. Chem. Soc.*, 1988, **110**, 4983; (*b*) W. J. Evans, K. A. Miller, S. A. Kozimor, J. W. Ziller, A. G. DiPasquale and A. L. Rheingold, *Organometallics*, 2007, **26**, 3568.
34 U. Bayer and R. Anwander, *Dalton Trans.*, 2020, **49**, 17472.
35 (*a*) D. Heitmann, C. Jones, D. P. Mills and A. Stasch, *Dalton Trans.*, 2010, **39**, 1877; (*b*) D. Werner, G. B. Deacon and P. C. Junk, *Inorg. Chem.*, 2019, **58**, 1912; (*c*) D. Toniolo, A. R. Willauer, J. Andrez, Y. Yang, R. Scopelliti, L. Maron and M. Mazzanti, *Chem.–Eur. J.*, 2019, **25**, 7831.
36 (*a*) D. Cui, M. Nishiura, O. Tardif and Z. Hou, *Organometallics*, 2008, **27**, 2428; (*b*) D. W. Beh, W. E. Piers, I. del Rosal, L. Maron, B. S. Gelfand, C. Gendy and J. B. Lin, *Dalton Trans.*, 2018, **47**, 13680.

37 (*a*) N. W. Davies, A. S. Frey, M. G. Gardiner and J. Wang, *Chem. Commun.*, 2006, 4853; (*b*) G. B. Deacon, P. C. Junk, J. Wang and D. Werner, *Inorg. Chem.*, 2014, **53**, 12553; (*c*) M. Xemard, V. Goudy, A. Braun, M. Tricoire, M. Cordier, L. Ricard, L. Castro, E. Louyriac, C. E. Kefalidis, C. Clavaguera, L. Maron and G. Nocton, *Organometallics*, 2017, **36**, 4660; (*d*) A. R. Willauer, D. Toniolo, F. Fadaei-Tirani, Y. Yang, M. Laurent and M. Mazzanti, *Dalton Trans.*, 2019, **48**, 6100; (*e*) A. R. Willauer, A. M. Dabrowska, R. Scopelliti and M. Mazzanti, *Chem. Commun.*, 2020, **56**, 8936.
38 J. Andrez, G. Bozoklu, G. Nocton, J. Pecaut, R. Scopelliti, L. Dubois and M. Mazzanti, *Chem.–Eur. J.*, 2015, **21**, 15188.
39 A. Paparo, J. S. Silvia, C. E. Kefalidis, T. P. Spaniol, L. Maron, J. Okuda and C. C. Cummins, *Angew. Chem., Int. Ed.*, 2015, **54**, 9115.